A practical nonlocal model for heat transport in magnetized laser plasmas

Ph. D. Nicolaï,[a] J.-L. A. Feugeas, and G. P. Schurtz
Centre Laser Intense et Applications (UMR 5107), CEA-CNRS-Université Bordeaux 1, 33405 Talence cedex, France

(Received 8 November 2005; accepted 2 February 2006; published online 24 March 2006)

A model of nonlocal transport for multidimensional radiation magnetohydrodynamics codes is presented. In laser produced plasmas, it is now believed that the heat transport can be strongly modified by the nonlocal nature of the electron conduction. Other mechanisms, such as self-generated magnetic fields, may also affect the heat transport. The model described in this work, based on simplified Fokker-Planck equations aims at extending the model of G. Schurtz, Ph. Nicolaï, and M. Busquet [Phys. Plasmas **7**, 4238 (2000)] to magnetized plasmas. A complete system of nonlocal equations is derived from kinetic equations with self-consistent electric and magnetic fields. These equations are analyzed and simplified in order to be implemented into large laser fusion codes and coupled to other relevant physics. The model is applied to two laser configurations that demonstrate the main features of the model and point out the nonlocal Righi-Leduc effect in a multidimensional case. © *2006 American Institute of Physics*. [DOI: 10.1063/1.2179392]

I. INTRODUCTION

Within the framework of inertial confinement fusion (ICF), the transport of energy by electron conduction is an old but unresolved problem. A correct modeling of this process is essential for the analysis and simulations of laser-matter interaction and for target design. Parametric instabilities,[1,2] laser absorption,[3] energy redistribution inside the plasma,[4] hydrodynamic instabilities,[5,6] and hot spot formation from which the thermonuclear reactions propagate, are directly or indirectly sensitive to the electron heat conduction. Besides, the current construction of megajoule energy lasers relies on the employment and the development of predictive multidimensional codes. More specifically, the high gain target design, for the direct or indirect drive, is based on two- or three-dimensional (2D, 3D) radiation hydrodynamic codes. However, the electron conduction model implemented in the majority of these codes is based on Spitzer-Härm's[7] (S-H) theory. This theory tends to overestimate the heat fluxes under sharp temperature gradients induced by high laser intensities. Thus, in order to reproduce experimental data, the S-H flux must be artificially limited. This limitation varies from one experiment to another depending on the laser intensity and wavelength, the geometry, plane or spherical. The heat transport affects laser absorption, x-ray emission, and hydrodynamic velocities.

The nonlocality of the electron transport is often pointed out as the main reason for the failure of the S-H theory in sharp gradient conditions. The explanation is that the heat carrying electrons travel at a velocity two to three times higher than the mean velocity. As the collision mean free path (mfp) scales as the fourth power of the velocity, these electrons may be issued from remote locations (in units of the temperature gradient length) of the plasma. They induce a natural limitation of the heat flux and preheat ahead of the temperature gradient. Since the early 1980s,[8–14] various authors have proposed practical formulae for nonlocal electron conduction in laser created plasmas, most of which rely on a delocalization kernel. For this reason, such delocalization models encounter difficulties near the plasma boundary and are limited to the one-dimensional (1D) geometry. Moreover, though they agree reasonably well with Fokker-Planck calculations, they fail to reproduce actual measurements.

Multidimensional (2D, 3D) effects should certainly be evoked. The nonlocal model of Schurtz et al.,[13] based upon a simplified kinetic approach, is better suited for implementation in multidimensional hydrodynamic codes. This model does not involve the convolution integrals and it correctly reproduces Fokker-Planck simulations, both in 1D and 2D. Unfortunately, it does not account for an important feature of multidimensional plasma flows; that is, the self-generation of intense magnetic fields. These fields are known to strongly affect the electron transport. This work aims at generalizing the previous nonlocal model in the presence of magnetic fields, with the same hypotheses of a weak departure from the thermal equilibrium and the same constraint of easy implementation and fast execution in a multidimensional radiative hydrodynamic code.

The paper is organized as follows. In Sec. II, we recall the multidimensional nonlocal model from which our study starts. We point out the causes of the nonlocal nature of the electron transport and its influence on macroscopic quantities. In Sec. III, we present the nonlocal effects on the electric field as well as the electric field effect on the modification of the distribution function in the velocity space. The heat transport model accounting for magnetic fields is developed in Sec. IV. In Sec. V, two numerical applications are presented. The first one presents the properties of our model and checks its limits. The second one applies to a realistic 2D configuration, and presents the role of the magnetic effects on the temperature distributions using the local or the nonlocal transport models. We also highlight the nonlocal Righi-Leduc effect, which may yield a heat flux in regions free

[a]Electronic address: nicolai@celia.u-bordeaux1.fr

from any temperature gradient. Finally, Sec. VI summarizes the main results.

II. THE NONLOCAL MODEL

A formal way to obtain the diffusion equations in the multidimensional model relies on the kinetic equation for the evolution of the electron distribution function (EDF) in the phase space. At first, let us suppose a zero current condition and neglect the magnetic field. The kinetic equation is

$$\partial_t f_e + \mathbf{v}\cdot\nabla f_e - \frac{e\mathbf{E}}{m_e}\cdot\nabla_{\mathbf{v}} f_e = C_{ee} + C_{ei}, \tag{1}$$

where $-e$ is the electron charge, m_e is the electron mass, c is the speed of light, and C_{ee}, and C_{ei} are electron-electron and electron-ion collision operators, respectively. $\mathbf{E}$ is the self-consistent electric field.

The kinetic equation gives a complete and microscopic description of electron dynamics, but its numerical solution consumes too much computer time and memory. It is not possible to compute this equation for each iteration in a large hydrodynamic code. We have to simplify the system while keeping the main kinetic effects. First, we adopt a first-order expansion for the distribution function, assuming its small anisotropy:

$$f_e(\mathbf{r},\mathbf{v},t) = f_0(\mathbf{r},v,t) + \frac{\mathbf{v}}{v}\cdot\mathbf{f}_1(\mathbf{r},v,t). \tag{2}$$

The main effect in a nonlocal transport is the departure of the isotropic part of the distribution function from the Maxwellian.[18,19] The departure from the S-H flux comes from this deformation and not from the first-order expansion,(2) which is considered to be accurate enough to describe laser-created plasmas.[2,21,22]

Secondly, we assume a steady state regime for electrons; that is, the distribution function adjusts itself to the fluid conditions of density and temperature. Making use of the expansion (2) in Eq. (1), we obtain

$$\frac{v}{3}\nabla\cdot\mathbf{f}_1 - \frac{e\mathbf{E}}{3m_e v^2}\cdot\nabla_v(v^2\mathbf{f}_1) = C^0_{ee}(f_0), \tag{3}$$

$$v\nabla f_0 - \frac{e\mathbf{E}}{m_e}\nabla_v(f_0) = C^1_{ee} + C^1_{ei},$$

$$= C^1_{ee} - \nu_{ei}\mathbf{f}_1 \simeq -\nu^*_{ei}\mathbf{f}_1, \tag{4}$$

where $\nu_{ei}=[4\pi n_e e^4 Z\Lambda/m_e]/v^3$ is the electron-ion collision frequency. We assume isotropic Rosenbluth potentials in the right-hand side of Eq. (3). In the Lorentz gas approximation, that is, in the high-Z limit, the electron-electron collisions can be neglected compared with the electron-ion collisions. For low Z values, tabulated or analytical corrections can be used[15–17] to calculate the transport coefficients. In the thermal conductivity case, the following expression $(Z+0.24)/(Z+4.2)$ correctly fits the Z dependence and can be directly applied to the electron-ion frequency $\{\nu^*_{ei}=[(Z+4.2)/(Z+0.24)]\nu_{ei}\}$. Always with the purpose of simplification, $C^0_{ee}(f_0)$ could be replaced by the Bhatnagar-Gross-Krook[23] operator. This latter is $\nu_{ee}(f_0-f_0^m)$, where $\nu_{ee}=[4\pi n_e e^4\Lambda/m_e]/v^3$ is the electron-electron collision frequency and f_0^m is the Maxwellian function, $f_0^m=n_e(m_e/2\pi T_e)^{3/2}e^{-m_e v^2/2T_e}$. Although simple, this operator leads to one of the best models of Luciani *et al.* [see Eq. (40) of Ref. 12 or Eq. (26) of Ref. 13]. In the high-velocity approximation, other collision operators could be used. Thus, the Albritton operator, which is $\nu_{ee}v\partial(f_0-f_0^m)/\partial v$, introduces diffusion in the velocity space and leads to a correct but more complicated model using several nonlocal propagators.[10,11]

Equation (4) gives us $\mathbf{f}_1$ and allows one to calculate the heat flux:

$$\mathbf{Q} = \frac{2\pi m_e}{3}\int_0^\infty \mathbf{f}_1 v^5 dv$$

$$= -\frac{2\pi m_e}{3}\int_0^\infty \left[v\nabla f_0 - \frac{\mathbf{eE}}{m_e}\nabla_v(f_0)\right]\frac{v^5}{\nu^*_{ei}}dv, \tag{5}$$

where the electric field is given by the zero current condition

$$\mathbf{J} = -\frac{4\pi e}{3}\int_0^\infty \mathbf{f}_1 v^3 dv = 0,$$

$$\Rightarrow \mathbf{E} = -\frac{m_e}{6e}\frac{\int_0^\infty \nabla f_0 v^7 dv}{\int_0^\infty f_0 v^5 dv}. \tag{6}$$

The classical Spitzer-Härm theory follows from Eq. (6), if we postulate that f_0 is a Maxwellian function. Thus,

$$\mathbf{E}^m = -\frac{T_e}{e}\left(\frac{\nabla n_e}{n_e} + \zeta\frac{\nabla T_e}{T_e}\right), \tag{7}$$

where ζ is a function of Z. Using the Spitzer-Härm notation,[7] $\zeta=\left[1+\frac{3}{2}\gamma_T/\gamma_E\right]$. ζ ranges from 1.7 ($Z=1$) to 2.5 ($Z=\infty$). Inserting the electric field into the heat flux formula leads the Spitzer-Härm flux. Note that the Z dependence of the electric field (ζ) no longer appears in the heat flux formula due to compensating effects.[7] The only remaining Z dependence of the heat flux can be correctly described by a multiplicative factor as $(Z+0.24)/(Z+4.2)$. The integrand of the Spitzer-Härm heat flux is

$$\mathbf{f}_1^m = -\frac{v}{\nu^*_{ei}}\left(\frac{m_e v^2}{2T_e} - 4\right)f_0^m\frac{\nabla T_e}{T_e}. \tag{8}$$

Assume now that the EDF is not a Maxwellian function but remains close to it:

$$f_0 = f_0^m + \Delta f_0, \quad \mathbf{f}_1 = \mathbf{f}_1^m + \Delta\mathbf{f}_1. \tag{9}$$

Note that a departure of the distribution function from the Maxwellian could not be too large, in which case a fluid treatment would no longer be valid. Only high-order velocity moments as a heat flux may be strongly modified by kinetic effects. The density, mean velocity, or temperature have to be slightly affected by this perturbation. Inserting the EDF (9)

into Eqs. (3), (4), and (6), one obtains the following equations for Δf_0, $\Delta \mathbf{f}_1$, and $\Delta \mathbf{E}$:

$$-\nu_{ee}\Delta f_0 - \frac{v}{3}\nabla\cdot\Delta\mathbf{f}_1 + \frac{e\mathbf{E^m}}{3m_e v^2}\cdot\nabla_v(v^2\Delta\mathbf{f}_1) + \frac{e\Delta\mathbf{E}}{3m_e v^2}\cdot\nabla_v(v^2\mathbf{f}_1^m) + \frac{e\Delta\mathbf{E}}{3m_e v^2}\cdot\nabla_v(v^2\Delta\mathbf{f}_1) = + \frac{v}{3}\nabla\cdot\mathbf{f}_1^m - \frac{e\mathbf{E^m}}{3m_e v^2}\cdot\nabla_v(v^2\mathbf{f}_1^m), \tag{10}$$

$$-v\nabla\Delta f_0 + \frac{\mathbf{e}E^m}{m_e}\nabla_v(\Delta f_0) - \nu_{ei}^*\Delta\mathbf{f}_1 + \frac{e\Delta\mathbf{E}}{m_e}\nabla_v(f_0^m) + \frac{e\Delta\mathbf{E}}{m_e}\nabla_v(\Delta f_0) = 0, \tag{11}$$

and from the zero current condition,

$$\int_0^\infty\left[-v\nabla\Delta f_0 + \frac{\mathbf{e}E^m}{m_e}\nabla_v(\Delta f_0) + \frac{e\Delta\mathbf{E}}{m_e}\nabla_v(f_0^m) + \frac{e\Delta\mathbf{E}}{m_e}\nabla_v(\Delta f_0)\right]v^6dv = 0. \tag{12}$$

Note that a difference on the EDF induces a deviation of electric field from the local field ($\mathbf{E}=\mathbf{E}^m+\Delta\mathbf{E}$), which is described by Eq. (12). This last one could be written more simply as

$$\mathbf{E} = \mathbf{E}^m - \frac{m_e}{6e}\frac{\int_0^\infty\nabla\Delta f_0 v^7dv}{\int_0^\infty(f_0^m+\Delta f_0)v^5dv} - \frac{\mathbf{E}^m\int_0^\infty\Delta f_0 v^5dv}{\int_0^\infty(f_0^m+\Delta f_0)v^5dv}. \tag{13}$$

The evolution of the anisotropic part of the deformation follows from (11):

$$\mathbf{f}_1 = \mathbf{f}_1^m - \lambda_{ei}\nabla\Delta f_0 - \frac{\lambda_{ei}}{T_e}e\Delta\mathbf{E}f_0^m + \frac{\lambda_{ei}}{m_e v}e(\mathbf{E}^m+\Delta\mathbf{E})\nabla_v\Delta f_0, \tag{14}$$

where $\lambda_{ei}=v/\nu_{ei}=v^4m_e/[4\pi n_e e^4\Lambda]$ is the electron mean free path.

This last equation enables one to better understand the causes of the departure of f_1 from the Spitzer-Härm model. The first correction comes from the gradient of the isotropic part of the EDF deformation. It is proportional to the distance traveled by heat-carrying electrons. This term induces the preheat foot ahead of the temperature gradient. A perturbation of f_0, Δf_0, causes a perturbation of the electric field $\Delta\mathbf{E}$, which in turn acts on f_0. This effect appears in the second term. The third one gives the effect of total electric field on Δf_0. As we shall show in the next section, the first and last terms in Eq. (14) have opposite effects on nonlocal flux.

The set of kinetic equations for Δf_0, $\Delta\mathbf{f}_1$, and $\Delta\mathbf{E}$ can be solved and implemented into hydrodynamic codes, but it still remains complicated. Following Ref. 13, we simplify the model by keeping the dominant terms involving gradients and we account for the electric field corrections through the mean free path and a reduced source term in place of the right-hand side of Eq. (10). The new set of equations reduces to

$$\nu_{ee}\Delta f_0 + \frac{v}{3}\nabla\cdot\Delta\mathbf{f}_1 = -\frac{v}{3}\nabla\cdot\mathbf{g}_1^m, \tag{15}$$

$$v\nabla\Delta f_0 + \nu_{ei}^E\Delta\mathbf{f}_1 = 0, \tag{16}$$

where $\mathbf{g}_1^m=\lambda_{ei}^E f_0^m\nabla T_e/T_e$, the source term, mainly differs from Eq. (8) by the absence of the electron return current [formulae (21) and (22) of Ref. 13]. These slow electrons do not participate to delocalization fluxes and are not taken into account in equations. λ_{ei}^E is the electron mean free path limited by electric field. We suppose that an electron of energy E_g can travel no more than the distance E_g/eE [Eq. (35) of Ref. 13]. Now, inserting Eq. (16) into Eq. (15), one obtains a diffusive equation which could be quickly solved by any hydrodynamic codes disposing of an efficient diffusion solver. The integration of the fifth velocity momentum of Eq. (16) yields the formula for the heat flux:

$$\mathbf{Q} = \frac{2\pi m_e}{3}\int_0^\infty\mathbf{f}_1v^5dv = \frac{2\pi m_e}{3}\int_0^\infty\mathbf{f}_1^mv^5dv - \frac{2\pi m_e}{3}\int_0^\infty\lambda_{ei}^E\nabla\Delta f_0v^5dv. \tag{17}$$

The multidimensional nonlocal model retains the most important features of kinetic effects, which are: the flux limitation, the preheat and the rotation of heat flux vector with regard to the S-H flux. It has been successfully compared to 1D and 2D Fokker-Planck codes[13,24] and its diffusive form enables an easy implementation into hydrodynamic codes. It has been successfully introduced into large ICF codes as HYDRA[1] at the Livermore laboratory, LILAC[24] and ORCHID[25] at the Rochester laboratory and FCI2[4,13] at the CEA.

III. CLASSICAL AND NONLOCAL ELECTRIC FIELDS

Under electron temperature gradient, electrons move from the warm zone towards the cold one. A space charge appears, inducing an electric field that strives to ensure the plasma neutrality and to maintain a zero current. The electric field acts on heat flux carrying electrons, coming from hot part, by slowing down them. Electrons originating from the cold region also feel the effect of the field and move towards the hot part. The same number of particles moves in the two opposite directions, resulting in preservation of plasma neutrality. However, electrons coming from the warm zone are faster than those originating from the cold zone. It results in an energy transport between zones; that is, a heat flux. The Spitzer-Härm anisotropic term in the distribution function accounts for the return current, through the bracketed term in Eq. (8). In our reduced set of equations, deduced from the fact that the flux is carried by the high-velocity electrons, the current carried by cold electrons is neglected. This shifts down the maximum of the velocity distribution in the integrand in Eq. (17). We show in Fig. 1 that the maximum

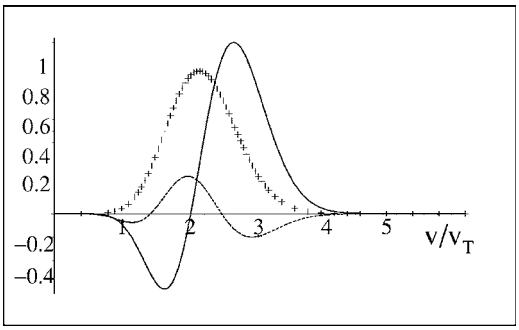

FIG. 1. Velocity dependence of the Spitzer-Härm integrand $v^5\mathbf{f}_1^m \propto (v/v_T)^9[(v/v_T)^2-4]\exp[-(v/v_T)^2]$ (solid curve), of the simplified source $v^5\mathbf{g}_1^m v^5 \propto (v/v_T)^9\exp[-(v/v_T)^2]$ (crosses), and of the electric field effect $\propto (v_T/v)^3\nabla_v\{(v/v_T)^6[(v/v_T)^2-4]\exp[-(v/v_T)^2]\}$ (dashed curve).

passes from $2.62v_T$ ($v_T=\sqrt{2T_e/m_e}$) for $v^5\mathbf{f}_1^m$ to $2.12v_T$ for the reduced source term $v^5\mathbf{g}_1^m$. Notice that this shift expresses an electric field effect in the nonlocal case. The classical correction due to electric field: $e\mathbf{E}^m/(3m_ev^2)\cdot\nabla_v(v^2\mathbf{f}_1^m)$ appears on the right-hand side in Eq. (10). This term produces after integration the Joule heating ($\mathbf{J}\cdot\mathbf{E}$), which vanishes because of the zero current condition. However, the Joule term contribution in each velocity group is not necessary null (Fig. 1). We obtain a positive contribution between $1.41v_{\text{th}}$ and $2.44v_{\text{th}}$ and negative above, leading to a velocity shift of the heat carrying electrons. In addition, as the nonlocality increases, the flux is carried by slower, more collisional electrons, causing a reduction of flux itself. At the beginning of the 1990s, Epperlein showed this effect numerically, using a Fokker-Planck code.[20] More recently, this behavior was put into evidence from a quasi-self-similar theory of electron kinetics.[26] Within the framework of a nonlocal computation, shifting the leading velocity is necessary, and this partly justifies the choice of our reduced source term. Besides, in the case of very large delocalizations, corresponding to a low collisionality, the electric field effect appears through the mean free path reduction. This limitation, which uses the stopping length due to electric field, acts in the hot and underdense regions as laser corona for instance, as shown in Ref. 27. Last, we can easily demonstrate by using a Fourier transform, that the introduction of electric field leads to the desired linear asymptotic behavior for the collisionless limit.[13]

The set of simplified equations (15) and (16) correctly reproduces the electric field effect on heat flux delocalization. Moreover, knowing Δf_0, one can calculate the electric field from Eq. (13). The classical S-H field, the nonlocal corrections, and the resulting electric field are shown in Fig. 2. Due to a lower velocity momentum, the deviation of electric field from the local field usually remains small, even under sharp gradient conditions. Note that the main difference does not necessary occur at the maximum of the electric field but happens near the edge of the transport zone due to the presence of nonlocal electrons there.

IV. THE EFFECTS OF THE MAGNETIC FIELD

Let us account for the magnetic fields in the kinetic equation

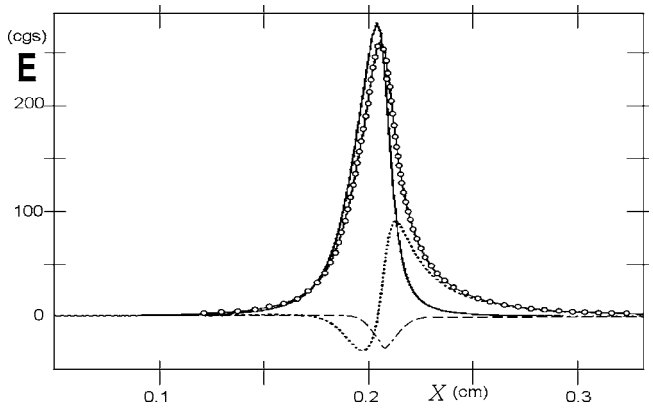

FIG. 2. Classical electric field (solid), the nonlocal electric field (empty circle), and the first (dotted) and second correction (dashed) in Eq. (13) in a nonlocal case: the delocalization parameter (see Refs. 8–13) $k\lambda_e \simeq 0.05$.

$$\delta_t f_e + \mathbf{v}\cdot\nabla f_e - e\left(\frac{\mathbf{E}}{m_e} + \mathbf{v}\times\frac{\mathbf{B}}{m_e c}\right)\cdot\nabla_{\mathbf{v}} f_e = C_{ee} + C_{ei}. \quad (18)$$

Following the same reasoning, we decompose the original equation in several equations giving the evolution of the isotropic and anisotropic parts of the EDF. Equation (3) remains unchanged, whereas Eq. (4) reads as

$$v\,\nabla f_0 - \frac{e\mathbf{E}}{m_e}\nabla_v(f_0) - \frac{e\mathbf{B}}{m_e c}\times\mathbf{f}_1 = -\nu_{ei}^*\mathbf{f}_1. \quad (19)$$

The solution to Eq. (19) is straightforward:

$$\mathbf{f}_1 = \frac{1}{\nu_{ei}^{*2}+\omega^2}\left[-\nu_{ei}^* v\,\nabla f_0 - v\,\boldsymbol{\omega}\mathbf{b}\times\nabla f_0 + \nu_{ei}^*\frac{e\mathbf{E}}{m_e}\nabla_v(f_0) + \boldsymbol{\omega}\mathbf{b}\times\frac{e\mathbf{E}}{m_e}\nabla_v(f_0)\right], \quad (20)$$

where $\omega = eB/m_e c$ is the electron gyrofrequency and $\mathbf{b} = \mathbf{B}/B$ is the unit vector in magnetic field direction.

Under this form, one can already foresee the effects of magnetic fields. As shown in the previous section, without $\mathbf{B}$, the anisotropic part comes from gradients in real space corrected by electric field effect. With B, we find again these terms, but rotated by the Lorentz force. Thus, $\mathbf{f}_1$ and thus the heat flux depends on gradients and fields along various directions due to the rotation of electrons under the magnetic field effect. One can have a flux even in a direction where there is no gradient. Another feature clearly appears in expression (20). Due to the division by $\nu_{ei}^{*2}+\omega^2$, the first and the third terms in brackets of Eq. (20) decrease strongly as $\mathbf{B}$ increases, whereas, after a passage through a maximum, the second and the fourth ones decrease more weakly.

In the difference from previous case, the condition of zero current has to be replaced by the Ampere-Maxwell's law:

$$-\frac{4\pi e}{3}\int_0^\infty \mathbf{f}_1 v^3 dv = \mathbf{J} = \frac{c}{4\pi}\nabla\times\mathbf{B}, \quad (21)$$

and Faraday's equation for the magnetic field, $(-1/c)\times(\partial B/\partial t) = \nabla\times\mathbf{E}$. Under this form, the equations are self-

consistent and a modification of the isotropic part of the EDF induces deviations on $\mathbf{f}_1$ and on the electromagnetic fields.

A. The Maxwellian distribution function case

To better understand the non-Maxwellian effects, it is interesting to begin with the simplest case, the Maxwellian electron distribution function. One can use the Lorentz gas approximation, which does not modify the physical behavior and could be widened by using appropriate coefficients.[16,17] These assumptions enable us to calculate analytically the anisotropic part of the EDF and all transport coefficients. We can thus express $\mathbf{f}_1^m$ as a function of the current and the temperature gradient:

$$\mathbf{f}_1^m = -C_\perp(v,\Omega)\frac{\mathbf{J}}{v_T e n_e} - C_\wedge(v,\Omega)\mathbf{b}\times\frac{\mathbf{J}}{v_T e n_e} - D_\perp(v,\Omega)\frac{v_T}{\nu_T}\frac{\nabla T_e}{T_e} - D_\wedge(v,\Omega)\mathbf{b}\times\frac{v_T}{\nu_T}\frac{\nabla T_e}{T_e}. \tag{22}$$

The four coefficients read as

$$\begin{aligned}
C_\perp(v,\Omega) &= \frac{u^4\phi_7 + \Omega^2 u^7\phi_{10}}{\phi_7^2+\Omega^2\phi_{10}^2}\frac{f_0^m}{1+\Omega^2u^6},\\
C_\wedge(v,\Omega) &= \frac{u^7\phi_7 - u^4\phi_{10}}{\phi_7^2+\Omega^2\phi_{10}^2}|\mathbf{\Omega}|\frac{f_0^m}{1+\Omega^2u^6},\\
D_\perp(v,\Omega) &= \left[\frac{u^6(\phi_7^2+\Omega^2\phi_{10}^2) - u^4(\phi_7\phi_9+\Omega^2\phi_{10}\phi_{12})}{\phi_7^2+\Omega^2\phi_{10}^2}\frac{+u^7(\phi_7\phi_{12}-\phi_{10}\phi_9)\Omega^2}{\phi_7^2+\Omega^2\phi_{10}^2}\right]\frac{f_0^m}{1+\Omega^2u^6},\\
D_\wedge(v,\Omega) &= \left[\frac{u^9(\phi_7^2+\Omega^2\phi_{10}^2) - u^4(\phi_7\phi_{12}-\phi_{10}\phi_9)}{\phi_7^2+\Omega^2\phi_{10}^2}\frac{-u^7(\phi_7\phi_9+\Omega^2\phi_{10}\phi_{12})\Omega^2}{\phi_7^2+\Omega^2\phi_{10}^2}\right]|\mathbf{\Omega}|\frac{f_0^m}{1+\Omega^2u^6},
\end{aligned} \tag{23}$$

where $u=v/v_T$, $\nu_T=\sqrt{2}\pi n_e Z e^4\Lambda/m_e^{1/2}T_e^{3/2}$ is the mean collision frequency and $\Omega=\omega/\nu_T$ is the Hall parameter, which accounts for the magnetic field influence on the transport coefficients. Finally, ϕ_n is a velocity integral, which reads as

$$\phi_n = \frac{4}{3\sqrt{\pi}}\int_0^\infty \frac{u^n e^{-u^2}du}{1+\Omega^2u^6}. \tag{24}$$

In order to obtain the heat flux, we have to calculate the integral of the fifth velocity momentum of Eq. (22). Using the notation adopted by Braginskii,[16] we write it as

$$\mathbf{Q}_B = -\beta_\perp\frac{T_e}{e}\mathbf{J} - \beta_\wedge\frac{T_e}{e}\mathbf{b}\times\mathbf{J} - \frac{5}{2}\frac{T_e}{e}\mathbf{J} - \kappa_\perp\nabla\mathbf{T_e} - \kappa_\wedge\mathbf{b}\times\nabla\mathbf{T_e}, \tag{25}$$

where $\beta_{\perp,\wedge}$ and $\kappa_{\perp,\wedge}$ are the components of the thermoelectric and thermal conductivity tensors, respectively:

$$\begin{aligned}
\beta_\perp &= \frac{\phi_9\phi_7+\Omega^2\phi_{12}\phi_{10}}{\phi_7^2+\Omega^2\phi_{10}^2} - \frac{5}{2},\\
\beta_\wedge &= \frac{\phi_{12}\phi_7-\phi_9\phi_{10}}{\phi_7^2+\Omega^2\phi_{10}^2}|\mathbf{\Omega}|,\\
\kappa_\perp &= \frac{2T_e n_e}{m_e\nu_T}\frac{(\phi_{11}\phi_7^2-\phi_7\phi_9^2)+\Omega^2(\phi_{11}\phi_{10}^2+\phi_7\phi_{12}^2-2\phi_9\phi_{10}\phi_{12})}{\phi_7^2+\Omega^2\phi_{10}^2},\\
\kappa_\wedge &= \frac{2T_e n_e}{m_e\nu_T}|\mathbf{\Omega}|\cdot\frac{(\phi_{14}\phi_7^2+\phi_{10}\phi_9^2-2\phi_7\phi_9\phi_{12})+\Omega^2(\phi_{14}\phi_{10}^2-\phi_{10}\phi_{12}^2)}{\phi_7^2+\Omega^2\phi_{10}^2}.
\end{aligned} \tag{26}$$

These formulae account for the corrections by Epperlein and Haines,[17] who found an error of up to 65% in the Braginskii coefficients. $\mathbf{Q}_B$ and $\mathbf{f}_1$ have similar structures and the first analysis given for Eq. (20) also applies to Eqs. (22) and (25). Thus, a temperature gradient perpendicular to a magnetic field induces a flux in the gradient direction (denoted $\perp$) and a flux in a crossed direction (denoted $\wedge$). This last one is the Righi-Leduc term. The electron rotation due to B fields leads to current loops acting on fluxes. The third term on the right-hand side of Eq. (25) represents the enthalpy energy flow, which depends on the reference frame.

In the same way, the electric field has the following form:

$$e\mathbf{E}_B = -\frac{\nabla P_e}{n_e} + \frac{\mathbf{J}\times\mathbf{B}}{n_e c} - \beta_\perp \nabla T_e - \beta_\wedge \mathbf{b}\times\nabla T_e + \alpha_\perp \frac{\mathbf{J}}{n_e^2} - \alpha_\wedge \mathbf{b}\times\frac{\mathbf{J}}{n_e^2}, \tag{27}$$

where P_e is the electron pressure. The electrical resistivity terms are defined by

$$\alpha_\perp = \frac{n_e m_e \nu_T}{2}\frac{\phi_7}{\phi_7^2+\Omega^2\phi_{10}^2},$$

$$\alpha_\wedge = \frac{n_e m_e \nu_T}{2}\left(1-\frac{\phi_{10}}{\phi_7^2+\Omega^2\phi_{10}^2}\right)|\mathbf{\Omega}|. \tag{28}$$

The first term in the right-hand side of Eq. (27) is the main source of large-scale magnetic fields in ICF plasmas. The second one is known as the Hall term. The forth term yields the Nernst contribution. Substituting Eq. (27) into Faraday's law, one obtains the equation for the magnetic field evolution; i.e., the source terms, the magnetic convection, the resistive diffusion, the magnetic curvature, and thermal force terms. In the limit of a zero magnetic field, $\mathbf{f}_1$ tends towards Eq. (8) the Spitzer-Härm integrand, the electric field is reduced to Eq. (7) and the Braginskii fluxes degenerate to the Spitzer-Härm fluxes.

B. The non-Maxwellian distribution function case

In the Maxwellian case, although some terms are difficult to discretize, all could be taken into account in a large magnetohydrodynamic code. In the non-Maxwellian distribution function case, the complexity increases and some approximations must be made. We split the EDF as $f_0=f_0^m+\Delta f_0$ and $\mathbf{f}_1=\mathbf{f}_1^m+\Delta\mathbf{f}_1$. The kinetic equations become

$$-\nu_{ee}\Delta f_0 - \frac{v}{3}\nabla\cdot\Delta\mathbf{f}_1 + \frac{e\mathbf{E_B}}{3m_e v^2}\cdot\nabla_v(v^2\Delta\mathbf{f}_1) + \frac{e\Delta\mathbf{E}}{3m_e v^2}\cdot\nabla_v(v^2\mathbf{f}_1^m) + \frac{e\Delta\mathbf{E}}{3m_e v^2}\cdot\nabla_v(v^2\Delta\mathbf{f}_1) = +\frac{v}{3}\nabla\cdot\mathbf{f}_1^m - \frac{e\mathbf{E_B}}{3m_e v^2}\cdot\nabla_v(v^2\mathbf{f}_1^m), \tag{29}$$

$$-v\nabla\Delta f_0 + \frac{\mathbf{e}E_B}{m_e}\nabla_v(\Delta f_0) - \nu_{ei}^*\Delta\mathbf{f}_1 + \frac{e\Delta\mathbf{E}}{m_e}\nabla_v(f_0^m) + \frac{e\Delta\mathbf{E}}{m_e}\nabla_v(\Delta f_0) + \omega\mathbf{b}\times\Delta\mathbf{f}_1 + \Delta\omega\mathbf{b}\times\mathbf{f}_1^m + \Delta\omega\mathbf{b}\times\Delta\mathbf{f}_1 = 0, \tag{30}$$

where $\mathbf{f}_1^m$ is not the S-H integrand but the more complicated Braginskii integrand given by Eq. (22). A deformation of the EDF induces a variation on the electromagnetic fields which in turn could affect the EDF. Although less complex than a 2D-3D Fokker-Planck code, the resolution of these equations would lead to computing times making prohibitive any calculation. We suggest to reduce this set of equations while keeping the main effects.

In this purpose, several arguments can be advanced. First, the deformations of the EDF (Δf_0 and $\Delta\mathbf{f}_1$) come from kinetic effects due to the long electron mean free path compared to the temperature gradient length. These deformations affect more significantly the high-energy electrons, which modify the high-velocity momenta like the heat fluxes. For lower momenta, the deformation effects are less important. For this reason, the perturbation of electric and magnetic fields is not too important, as shown in the Fig. 2 for the E field.

On the other hand, electric and magnetic fields tend to reduce the nonlocal effects. This behavior for electric field was already discussed in a previous section and also shown in Refs. 13 and 27 in the laser corona case where the electric field has a strong influence. Concerning the magnetic fields, this reduction was pointed out in Refs. 4, 8, 28, and 29. Qualitatively, one can say that electrons traveling in the neighborhood of a field line are deflected by the Lorentz's force. Thus, in the primary direction, the apparent mean free path is reduced. Strong magnetic fields prevent electrons to move across the magnetic field lines, so that they cannot transport any flux. Lorentz's force is velocity dependent and induces a magnetization of high-speed electrons, which are also carriers of the heat flux. An indication of this effect can be simply given by comparing the mean free path of the heat-carrying electrons with the Larmor radius, which gives the radius of gyration of electrons subject to a magnetic field ($u^3\mathbf{\Omega}$). In conclusion, a small departure due to a nonlocal effect remains small or becomes even smaller when one takes into account the magnetic fields.

Thus, the previous results based on a weak departure from the locality could be extended to the case with magnetic fields. We suggest the following set of equations for the non-Maxwellian correction of the EDF with reduced mean free path and corrected source term:

$$-\frac{3}{\lambda_{ee}}\Delta f_0 + \nabla\cdot\left\{\frac{\lambda_{ei}^*}{1+u^6\mathbf{\Omega}^2}[\nabla\Delta f_0 + u^3\mathbf{\Omega}\times\nabla\Delta f_0]\right\} = \nabla\cdot\mathbf{g}_1^m, \tag{31}$$

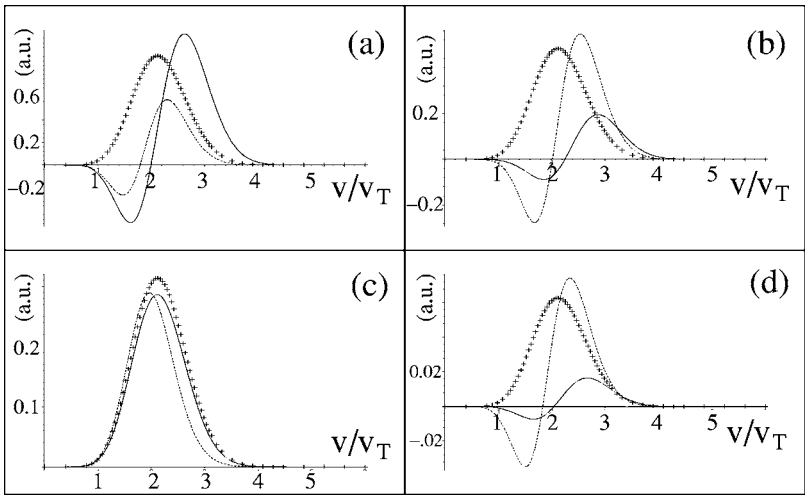

FIG. 3. Velocity dependence of $\mathbf{f}_1^m$ coefficients times v^5: $v^5D_\perp$ (a), $v^5D_\wedge$ (b), $v^5C_\perp$ (c), and $v^5D_\wedge$ (d) for $\Omega=0.01$ (solid line), 0.1 (dotted line), and 1.0 (gray line). Crosses refer to $v^5\mathbf{g}_1^m$.

$$\mathbf{f}_1 = \mathbf{f}_1^m - \frac{\lambda_{ei}^*}{1+u^6\mathbf{\Omega}^2}[\nabla\Delta f_0 + u^3\mathbf{\Omega}\times\nabla\Delta f_0]. \tag{32}$$

Equation (31) has a desired form of a diffusion equation. For $\Delta\mathbf{f}_1$, one retrieves the feature of Eq. (20) without the electric field dependence, but with the **B** influence. Both main characteristics, which we wanted to keep, appear in the $\Delta\mathbf{f}_1$ expression: the mean free path reduction, which scales as $1+u^6\mathbf{\Omega}^2$, and the rotation of electrons under the form $u^3\mathbf{\Omega}\times\nabla\Delta f_0$. On the other hand, $\mathbf{f}_1^m$, given by Eq. (22), already takes into account electric and magnetic fields. The electric field effect on the delocalized part can be corrected as shown without **B**, using a stopping length due to **E** field or in this case, the Larmor radius. We also use the same source term as Eq. (15). For the electrostatic case, this assumption was been justified in previous sections, and we have to check it in the electromagnetic field case. The fact of using $\mathbf{g}_1^m$ means that we suppose that B fields shift down the leading velocity too. We have drawn in the Fig. 3 the velocity dependence of coefficients, $(C_\perp, C_\wedge, D_\perp, D_\wedge)$ times v^5, which appear in the formula of $\mathbf{f}_1$ [Eq. (22)] for various values of Ω. These curves give the velocity contribution to the heat flux and are compared to $v^5\mathbf{g}_1^m$. After integration, these functions lead to the coefficients κ and β and thus follow their Ω dependence. We observe a sharp decrease for $D_\perp$ and a smoother one for $C_\perp$, while $D_\wedge$ and $C_\wedge$ start from zero, pass through a maximum close to $\Omega=0.1$, and then slowly decrease. As Ω and thus B increase as the main velocity contribution shifts down. For example, the maximum for $D_\perp$ passes from $2.61v_T$ for $\Omega=0.01$ to $1.93v_T$ for $\Omega=1$. The behavior is exactly the same as in the case without a magnetic field when the temperature gradient becomes sharper. One can therefore conclude that if $\mathbf{g}_1^m$ is a good approximation in the nonlocal case, it remains correct in the magnetic field case, and could be used as a source term in Eq. (31). Note that among the four coefficients presented in Fig. 3, one of them presents a different shape: $C_\perp$ does not have a negative part in the velocity space. Now as the order of the velocity momentum decreases, the contribution of the negative part increases and counterbalances the positive part. For this reason, the integration of $v^3D_\perp$, $v^3D_\wedge$, and $v^3C_\wedge$ gives zero, for all Ω, while $v^3C_\perp$ gives $3n_e/4\pi v_T^3$. One can easily check that the third velocity momentum yields Eq. (21).

One can improve the accuracy of the model and understand better the roles of various mechanisms. Assume first, that one only keeps the zeroth- and first-order terms in Eq. (30). Second, due to a low velocity momentum, suppose that $(\omega+\Delta\omega)\mathbf{b}\times\mathbf{f}_1^m$ could be approximated by $\omega\mathbf{b}\times\mathbf{f}_1^m$. Under these conditions, Eq. (30) reads

$$\begin{aligned}\mathbf{f}_1 = \mathbf{f}_1^m - \frac{\lambda_{ei}}{1+u^6\mathbf{\Omega}^2}\Bigg[&+\nabla\Delta f_0 + u^3\mathbf{\Omega}\times\nabla\Delta f_0 + \frac{e\Delta\mathbf{E}}{T_e}f_0^m \\ &+ \frac{u^3\mathbf{\Omega}\times e\Delta\mathbf{E}}{T_e}f_0^m - \frac{e\mathbf{E}_B}{m_e v_T^2 u}\nabla_u\Delta f_0 \\ &- \frac{u^3\mathbf{\Omega}\times e\mathbf{E}_B}{m_e v_T^2 u}\nabla_u\Delta f_0\Bigg].\end{aligned} \tag{33}$$

If **B** goes to zero, Eq. (33) reduces to Eq. (14) without the second-order term. The three additional terms could be analyzed in the same way as those without magnetic fields. The only difference comes from the rotation due to the Lorentz's force and, for all terms, from the mean free path reduction. One shows, through comparisons with Fokker-Planck codes,[13,24] that Eq. (14) is approximated very well by Eq. (16). As magnetic fields tend to reduce the nonlocal effects, Eq. (32) could be considered as a good approximation of Eq. (33) using the correct source term and a reduced mean free path. The electric fields that appear in Eq. (33) are those of Braginskii, and $\Delta\mathbf{E}$ is defined by an equation similar to Eq. (13):

$$\begin{aligned}e\mathbf{E} = e\mathbf{E}_B - \frac{m_e v_T}{\Upsilon_7^2(f_0^m)+\mathbf{\Omega}^2\Upsilon_{10}^2(f_0^m)}\Bigg\{&+ v_T\Upsilon_7(f_0^m)[\Upsilon_7(\nabla\Delta f_0) \\ &+ \mathbf{\Omega}\times\Upsilon_{10}(\nabla\Delta f_0)] - v_T\Upsilon_{10}(f_0^m)[\mathbf{\Omega}\times\Upsilon_7(\nabla\Delta f_0) \\ &- \Omega^2\Upsilon_{10}(\nabla\Delta f_0)] - \frac{e\Upsilon_7(f_0^m)}{v_T m_e}[\mathbf{E}_B\Upsilon_6(\nabla_u\Delta f_0) + \mathbf{\Omega} \\ &\times\mathbf{E}_B\Upsilon_9(\nabla_u\Delta f_0)] + \frac{e\Upsilon_{10}(f_0^m)}{v_T m_e}[\mathbf{\Omega}\times\mathbf{E}_B\Upsilon_6(\nabla_u\Delta f_0)\end{aligned}$$

$$-\Omega^2\mathbf{E}_B\Upsilon_9(\nabla_u\Delta f_0)]\Bigg\}, \tag{34}$$

where $\Upsilon_n(h)=\int_0^\infty u^n h du/(1+\Omega^2u^6)$ is an extension of Eq. (24): $\Upsilon_n(e^{-u^2})=(3\sqrt{\pi}/4)\phi_n$.

We verify that as **B** tends towards zero, Eq. (34) reduces to Eq. (13). Moreover, if **B** increases, nonlocal effects tend to vanish ($\Delta f_0\to 0$) and **E** reduces to $\mathbf{E}_B$.

Before closing this part, let us indicate that most of the velocity integrated quantities must be written differently for computational purposes. Formulae (14) and (33) aim at giving insight in the relationship between the deformation of the EDF and the delocalization of fields. However in a practical calculation, currents and fields can be computed in a straightforward manner from the nonlocal electron distribution function. In the absence of any magnetic fields, Eq. (6) yields the electric field. The field may be computed explicitly from the EDF known from the previous time step. With **B** fields, the electric field is given by the generalized Ohm's law:

$$e\mathbf{E}=\frac{m_e v_T^2}{\Upsilon_6^2(\nabla_u f_0)+\Omega^2\Upsilon_9^2(\nabla_u f_0)}\Bigg\{-\Upsilon_6(\nabla_u f_0)\Bigg[\frac{3\nu_T}{4\pi e v_T^5}\mathbf{J}+\mathbf{\Omega}\times\Upsilon_{10}(\nabla f_0)+\Upsilon_7(\nabla f_0)\Bigg]+\Upsilon_9(\nabla_u f_0)\Bigg[\frac{3\nu_T}{4\pi e v_T^5}\mathbf{\Omega}\times\mathbf{J}-\mathbf{\Omega}\times\Upsilon_7(\nabla f_0)+\Omega^2\Upsilon_{10}(\nabla f_0)\Bigg]\Bigg\}. \tag{35}$$

If f_0 is the Maxwellian, the above formula reduces towards Eq. (27). Otherwise, Eq. (35) exhibits, by identification, the nonlocal source term, as well as the nonlocal resistivity tensor, the nonlocal thermoelectric tensor and the nonlocal Nernst velocity. When **B** is given, the **E** field from Eq. (35) is the input for the nonlocal flux. For a self-consistent calculation of **B**, one has to substitute **J** by $c/4\pi\nabla\times\mathbf{B}$ in the previous equation and introduce the fluid velocity **u**. Thus, Faraday's law reads

$$\frac{\partial\mathbf{B}}{\partial t}+\nabla\times(\mathbf{u}\times\mathbf{B})=-c\,\nabla\times\mathbf{E}$$

This latter equation defines the time evolution of **B**. The transport coefficients may be calculated explicitly from the data originated from the previous time step. Conversely, all terms linear in **B** should be made implicit in the magnetohydrodynamic solver.

Thus, our approach takes into account the magnetic effects on nonlocal fluxes and in turn could modify the magnetic fields due to the nonlocal transport. Although usually small, because of the velocity momentum used and of the antinomy between a long mfp and magnetic fields, this modification could lead to surprising results. For example, as shown by R. Kingham and A. Bell,[22] the nonlocal transport could induce magnetic fields without a density gradient; that is, in the case where the classical calculation does not foresee any field. This effect is directly related to the electron distribution function deformation. More precisely, they have shown that the velocity dependence of the mfp may lead to an angle between the velocity moment gradients $[\nabla(\langle v^5\rangle)\times\nabla(\langle v^7\rangle)$ with $\langle v^n\rangle=\int_0^\infty v^n f_0 dv]$, which generates the magnetic field.

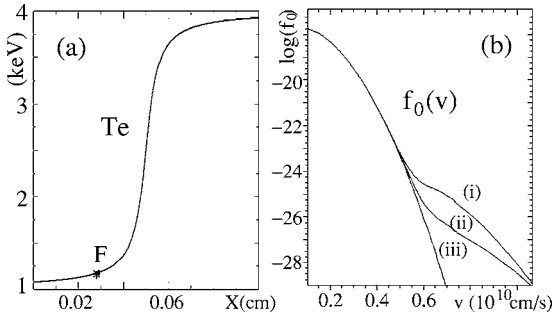

FIG. 4. (a) Temperature profile. (b) Isotropic part of the EDF at position F: (i) nonlocal without **B**, (ii) nonlocal with **B**, and (iii) Maxwellian.

V. NUMERICAL RESULTS

In order to compute, for every iteration of a 2D or 3D hydrodynamic code, the nonlocal heat fluxes as well as the other quantities as currents or electric fields, the system of equations (31) and (32) combined with Eqs. (22) and (27) is preferred to the complete set (29) and (30). This simplified set has been implemented into a 2D Lagrangian hydrodynamic code CHIC,[31] developed at our laboratory. The numerical scheme uses a nonsymmetric solver for crossed terms and a implicit-explicit method for counterstreaming fluxes. The principles of implementation are given in the Appendix.

A. The magnetic field effects in the 1D case

Let us consider a temperature profile [Fig. 4(a)], along the x axis, varying from 1.08 to 3.92 keV at the distance 60 μm, with a constant electron density equal to 10^{21} cm^{-3}. This gradient is sharp enough to introduce nonlocal effects: the corresponding delocalization parameter[8–13] $k\lambda_e$ is approximately equal to 0.08 [k is the logarithmic temperature gradient and λ_e equals $(Z+1)^{1/2}$ times the thermal mean free path]. A magnetic field, is directed along the z axis. Figures 5(a) and 6(a) show the fluxes colinear to the temperature gradient,while Figs. 5(b) and 6(b) present those that are per-

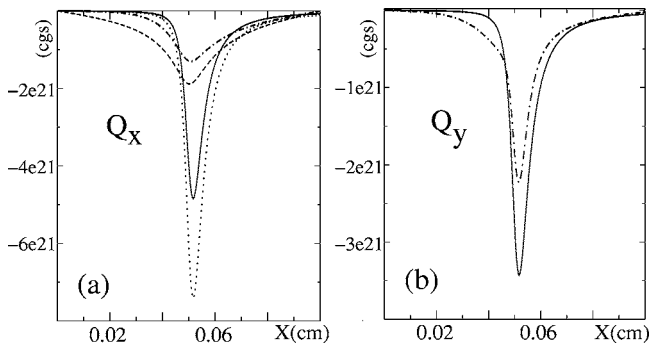

FIG. 5. Heat fluxes for $\Omega=0.1$ (a) fluxes colinear to the gradient; (b) fluxes perpendicular to the gradient; solid lines refer to Braginskii, dotted lines to Spitzer-Härm, dashed line to nonlocal, and dash-dotted lines to nonlocal with **B**.

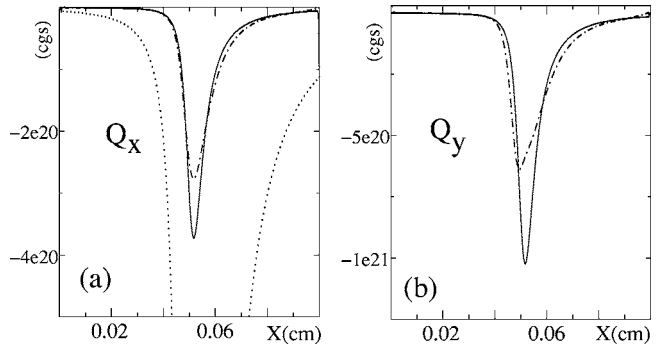

FIG. 6. Heat fluxes for $\Omega=1$. (a) Fluxes colinear to the gradient. (b) Fluxes perpendicular to the gradient. Solid lines refer to Braginskii, dotted lines to Spitzer-Härm, and dash-dotted lines to nonlocal with **B**.

pendicular to the gradient and to the magnetic field direction; that is, along the y axis. Without magnetic field, our fluxes agree with nonlocal results: a flux smaller than the local flux and a preheat foot ahead of the temperature gradient. The difference between both maxima is in agreement with the previous studies in the Fourier space using a Fokker-Planck code.[12] With magnetic field, new effects appear. Suppose, to simplify, a magnetic field such that Ω is constant and equals 0.1 (Fig. 5); that is, due to the temperature gradient, the magnetic field varies from 65.2 kG (cold part) to 12.9 kG (warm part). Both local and nonlocal fluxes are reduced. The reduction is less important for the nonlocal case due to a decrease of the electron mean free path inducing a relocalization of the flux. Secondly, the mean free path being smaller, the amount of energy brought ahead of the gradient is smaller. This last effect is enhanced by the Lorentz's force. Actually, a part of electrons is deviated towards the y direction and these latter no longer participate in the heat transport along the gradient. Nevertheless, although the fields reduce the nonlocal effects, the flux remains nonlocal and smaller than the local flux given by the Braginskii's formula. Consequently, in the perpendicular direction to the gradient, one obtains, after rotation, a smaller and enlarged flux relative to the Righi-Leduc local component. The competition between nonlocal and magnetic field effects has been studied in the past, by using the Fokker-Planck codes[22,29] or a linearized electron kinetic equation.[28] Our results could be compared with the previous ones, in the one-dimensional case. In particular, one can verify that our model agrees with the Brantov *et al.*[28] results, noting that the definition of Ω differs by the factor $3\pi^{1/2}/4$.

In the case of stronger magnetic field ($\Omega \simeq 1$), the fluxes are presented in Figs. 6(a) and 6(b). Note that the scales are strongly different. The heat conduction is strongly reduced and the energy is partially confined. The nonlocal effects are less important and our model reduces towards the Braginskii one. However, due to the Ω dependence in $u^3\mathbf{\Omega}/(1+u^6\mathbf{\Omega}^2)$, the nonlocal effect in the crossed term decreases more slowly to the Righi-Leduc component than the term parallel to the gradient. Thus, in this case, the model predicts a nonlocal transverse heat flux while the longitudinal flux remains local.

By construction, our model uses the departure of the EDF from the Maxwellian to build the heat flows. Thus, everywhere and at any time, we access Δf_0 and $\Delta \mathbf{f}_1$, and thus, f_0 and $\mathbf{f}_1$. We present on Fig. 4(b), an example of deformation of the isotropic part of the EDF with and without the magnetic field. The function is calculated in the point marked "F" in Fig. 4(a); that is, just ahead of the temperature gradient. The deformation of f_0 is due to the heat-carrying electrons coming from the hot part of plasma. As shown, the departure to the Maxwellian is strongly reduced by the presence of the magnetic field, showing the decrease of the mean free paths and thus of the nonlocal effects. The EDF could be used to compute other physical processes, such as the Landau damping of plasma wave or the x-ray emission. However, it is worthwhile to recall that the model was developed to reproduce the heat transport; that is, for suprathermal electrons having high velocities. In particular, the simplified collision operators ensure fast and correct heat flux simulations but poorly reproduce the distribution of low-velocity electrons. Only the high-energy part of the distribution function could be considered as quantitatively correct. For velocities smaller or equal to the mean velocity, the model predicts that electrons follow the velocity distribution of the local Maxwellian function. A better information requires a more accurate treatment of collisions; that is, the use of the Fokker-Planck equations.

B. Heat transport in a 2D laser configuration

The previous example illustrates some properties of the model, but does not intend to describe the effects in a plasma created by laser. Here, we consider a more realistic case. Suppose a solid planar target illuminated by laser. For a nanosecond pulse and for the intensity of $10^{14}-10^{15}$ W/cm^2, one obtains the electron temperatures above 1 KeV and ablation mass rates above 10^5 g/cm^2/s. Besides, under these conditions, at the edge of the laser focal spot, the gradients of density and temperature are noncolinear. This induces large self-generated magnetic fields of the intensity of a few megagauss.[4,32] Such fields affect the electron transport and thus the energy redistribution inside the plasma. A characteristic temperature map is given in Fig. 7(a). The laser comes from the right and the intensity is axially symmetric with respect to the z axis (we just draw the top half of the map). The temperature spatial distribution depends on the

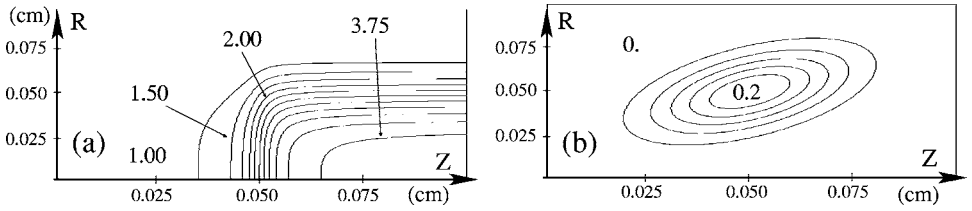

FIG. 7. (a) Isolevel curves of the temperature. The numbers are the temperature values in keV (the difference between two levels equals 250 eV) and (b) isolevel curves of Ω (the difference between two levels equals 0.04).

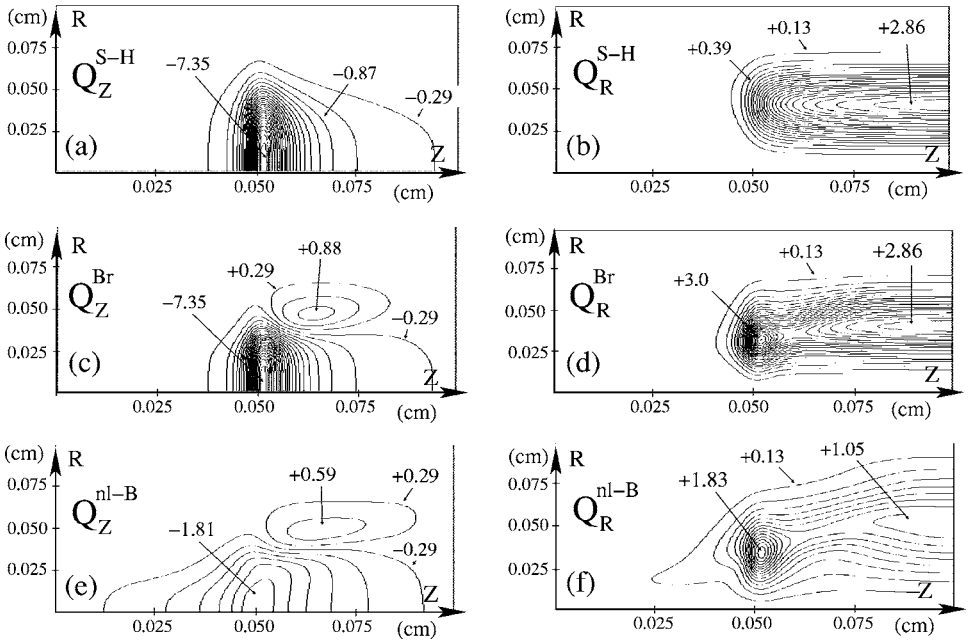

FIG. 8. Isolevel curves of the Spitzer-Härm fluxes (a) along the 0-Z axis and (b) in the radial direction; the Braginskii flux (c) along the 0-Z axis and (d) in the radial direction; (e) the fluxes given by our model (e) along the 0-Z axis and (f) in the radial direction. The fluxes are in 10^{21} erg/cm^2/s. The variation between two levels equals 0.2910^{21} erg/cm^2/s for the panels (a), (c), (e), and equals 0.1310^{21} erg/cm^2/s for the panels (b), (d), (f).

laser intensity profile and the heat conduction. As we assume the cylindrical geometry (R-Z), the magnetic fields are directed along the azimuthal direction (θ). The Ω map is shown in the Fig. 7(b) with a maximum close to 0.2. The temperature and omega values, the gradients lengths and the sizes of the simulation box are typical for the ICF conditions.

The classical Spitzer-Härm fluxes, without magnetic field, are presented in the Figs. 8(a) and 8(b) for both directions of the simulation. The fluxes which account for magnetic field, in the local case (the Braginskii fluxes) are shown in Figs. 8(c) and 8(d). For a given direction, the scale remains the same. Obviously, in the zone free from magnetic fields, the fluxes remain unchanged. Elsewhere, the flux component along the gradient is reduced, and the cross-component appears. This latter could enhance the existing flux along the R axis [Fig. 8(d)] or decrease it along the Z direction [Fig. 8(c)]. Figures 8(e) and 8(f) show, in the same scales as before, the fluxes given by our model. In the region free from **B** fields, because the gradients are sharp, the nonlocal features of the fluxes appear in both directions. As one approaches the zone of **B** influence, the nonlocal effects decrease. This particularly concerns the preheat along the Z direction. In addition the nonlocal cross-component appears. This latter, specifically in the R direction, is smaller and presents a slightly different shape due to the rotation of the electrons from the preheat foot. One can see that the combined effect of nonlocality and the self-generated magnetic field is important and cannot be ignored or described in local terms. One can easily understand that the use of Braginskii fluxes could improve simulation, but this is not sufficient in the region of sharp temperature gradients and free from magnetic fields. Conversely, a multidimensional nonlocal model alone which does not account for the magnetization of electrons can not reproduce the real fluxes in this simple laser configuration. Let us also indicate that the use of a flux limiter, as done in the most of hydrodynamic codes, puts various problems. Concerning S-H fluxes, the flux limiter has to report as well nonlocal as magnetic fields effects, which nevertheless lead to different limitations. Concerning Braginskii fluxes, one has to limit them only in weak **B**-field regions. Last, as shown by A. Sunahara *et al.*,[3] a time-dependent flux limiter is required to reproduce, in 1D, the nonlocal behavior at a given point inside the plasma. A flux limiter would depend on space and time and the best way to describe it is to consider a physical model of flux limitation.

We plot in Fig. 9 the temperature maps after 5 ps of a relaxation. Under these conditions, the S-H fluxes just smooth out temperature gradients and lead to the map shown in Fig. 9(b). Using the Braginskii fluxes, one obtains similar shapes except in the region of **B** influence. The main effect is a flux inhibition which leads to the energy confinement in this zone [Fig. 9(c)]. Our model, in Fig. 9(d), keeps the gradient sharp because the nonlocal flux is smaller than the S-H flux and induces a preheat ahead of gradient. In the zone of **B** influence, our model gets closer to Braginskii results, that is, becomes more local. However, the Righi-Leduc flux being stronger in the nonlocal case with regards to the flux along the temperature gradient, this effect can be seen in the temperature isolevel curves. Last, as already shown in previous studies,[13,33] the corona temperature remains hotter using the nonlocal model than the classical one.

VI. CONCLUSION

We have developed a multidimensional nonlocal model for the electron energy transport that accounts for self-generated magnetic fields. This model is derived from the kinetic Fokker-Planck equation, and it is reduced to the form

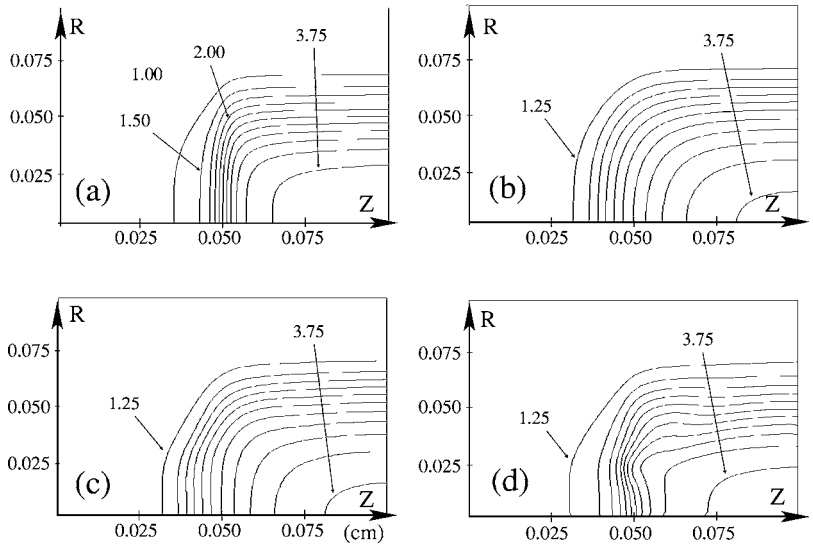

FIG. 9. (a) The isolevel curves of the initial temperature, and the final temperature after 5 ps using (b) the Spiter-Härm fluxes, (c) the Braginskii fluxes, and (d) our nonlocal model. The difference between two levels equals 250 eV.

of a nonlocal diffusion equation that is easily implementable into a large hydrodynamic code. The diffusive form is particularly adapted to these codes that dispose of efficient diffusion solvers. Our model accounts for, in two or three dimensions, the main characteristics of nonlocal nature of the heat conduction, namely, the flux inhibition, preheat, and counterstreaming flux, without paying the high computation cost of Fokker-Planck codes. In addition, our model is corrected by magnetic fields that could induce a flux inhibition, a flux rotation and a nonlocal effects cancelling. We have checked the model predictions in a realistic laser configuration, that is, in the presence of **B** fields and of sharp gradients, not necessarily at the same place. In the region free from magnetic field but under sharp gradient, it reduces to the nonlocal model of Ref. 13 which has been already checked and introduced into hydrodynamic codes. In the presence of intense magnetic fields, it reduces towards the Braginskii-Haines-Epperlein fluxes. Between both limits, it agrees in the 1D case, with previous monodimensional studies like that of Ref. 28. Thus, for the case where the fields are not too strong, the model accounts for a combination of magnetization and delocalization of the heat fluxes. Along the gradient, the flux is reduced by magnetic fields that render the flux more local: the departure from the Braginskii flux is reduced. Nevertheless, under the effect of the Lorentz's force, the Righi-Leduc-like term remains nonlocal. As the classical Righi-Leduc effect, the nonlocal Righi-Leduc effect produces a heat flux in the direction orthogonal to the gradient, but because of its nonlocal nature, this flux may exist in regions free from any gradient. The use of a flux limiter, although common in the hydrodynamic codes, cannot reproduce all these effects. Obviously, the preheating ahead of the temperature gradient cannot be correctly simulated, but in addition, the different limitations would require time-dependent multidimensional flux limiters. Last, to calculate the heat fluxes, our model evaluates the deformation of the electron distribution function, induced by heat transport and corrected by the magnetic fields. Thus, everywhere and at any time, we have access to the isotropic and anisotropic parts of the distribution function and thus to the modifications of all the quantities that are connected with it.

To summarize, this work proposes a multidimensional nonlocal model for heat transport in magnetized plasmas supposed to improve the simulations of ICF plasmas, the objective being to obtain a model fast enough to be introduced into a 2D or 3D code without making the simulation time prohibitive. The designs and the interpretations of laser experiments usually require the use of a multiphysics tool including not only the electron transport but also hydrodynamics, detailed radiation transport, nuclear burn, laser propagation, ionization, equations of state, and opacities. We believe that the present work contributes to improve the predictive capabilities of our numerical tools and our understanding of mechanisms governing the laser-produced plasmas.

ACKNOWLEDGMENTS

We acknowledge the fruitful comments of Vladimir Tikhonchuk on the manuscript. We are also grateful to Pierre-Henri Maire and Jerome Breil for their help in numerical implementation of the model. This work is partly supported by the Aquitaine Region council.

APPENDIX: NUMERICAL IMPLEMENTATION

We present in this part the general principles of the model implementation. The details are given elsewhere.[30] For simplicity, the analysis is carried out for the one group, unmagnetized case, and for a spatially uniform conductivity. One has to solve the energy equation, which is, neglecting hydrodynamics:

$$\rho C_v \frac{\partial T}{\partial t} + \nabla \cdot \mathbf{Q} = 0, \tag{A.1}$$

where C_v is the heat capacity.

In the local case, $\mathbf{Q}=-\kappa_{\mathrm{SH}}\nabla T$. For the purpose of stability analysis, Eq. (A.1) may be rewritten as $dT/dt=v_T\lambda_e d^2T/dx^2$. A given harmonic perturbation of the temperature field, in the form $T_k e^{ikx}$, will decay in time as $T_k(t)=T_k(0)e^{-v_T\lambda_e k^2 t}$. If Δt is the computational time step, an explicit time differencing of Eq. (A.1) will approximate the exponential decay factor by $1-v_T\lambda_e k^2\Delta t$, which will yield no decay at all when the time step becomes larger than $[v_T\lambda_e k^2]^{-1}$. The largest wave number a mesh of zone width h is able to sample is $2\pi/h$, which means that the maximum time step compatible with an explicit time differencing scales as $h^2/(v_T\lambda_e)$. In common ICF situations, one would obtain a time step lower than 10^{-15} s, which is not affordable for multinanosecond calculations. Conversely, the amplification factor of an implicit time differencing is $[1+v_T\lambda_e k^2\Delta t]^{-1}$, so that this latter scheme is stable for any time step.

After spatial differencing, the values of the temperature T in each cell are the solution of a linear set of equations in the form $AT^{n+1}=MC_vT^n$, where the subscript $n+1$ denotes the end of the time step, M the masses of cells, and A is a non-negative symmetric matrix. As the local flux operator only connects neighboring cells, A is sparse (tridiagonal in 1D, five diagonals in 2D when using a structured mesh of quadrangles), and its graph is constant in time. The equation is solved by means of LL^t factorization in 1D or preconditioned conjugate gradient iterations in 2D. Conversely, in the nonlocal case, the number of nonzero off-diagonal elements in A increases as the electron mean free path becomes larger. As this number is not *a priori* known, A must be considered as a full matrix, and the solution of the linear set of equations becomes much more expensive in terms of data storage and computing time. A crude solution has been proposed in the past to partly solve this problem.[9] The idea amounts to calculate an apparent thermal conductivity:

$$\mathbf{Q}=-\kappa_{\mathrm{nl}}\nabla T,\quad \text{with}\quad \kappa_{\mathrm{nl}}=\frac{\mathbf{Q}_{\mathrm{nl}}}{\nabla T},\tag{A.2}$$

and implicitly time-difference the energy equation. The method yields results close to those of the complete system and the CPU time gain is important. However, it suffers from severe drawbacks, mainly because an effective conductivity cannot be calculated in places where the temperature gradient is zero, nor in places where the temperature gradient has the same sign as the nonlocal heat flux; thus, neither fast electron preheat nor counterstreaming fluxes can be correctly predicted by the apparent conductivity approach.[9,13]

An important property of the nonlocal conduction allows us to circumvent this difficulty. If we perform the same Fourier analysis as previously, we obtain, in the one-group nonlocal case, the eigenfrequency of the nonlocal heat conduction operator:

$$\omega_{\mathrm{nl}}=\frac{\omega_{\mathrm{SH}}}{1+a(\lambda_e k)^\alpha}=\frac{v_T\lambda_e k^2}{1+a(\lambda_e k)^\alpha},\tag{A.3}$$

where a is a constant and $0.9<\alpha<2$. ($\alpha=2$ for the original Luciani kernel[8]). Hence, this frequency is bounded in the Luciani's case, and varies quasilinearly with $\lambda_e k$ in our nonlocal model case. For this reason, the stability criterion for an explicit time differencing is much less restrictive in the nonlocal case, as compared to the local case. For $\alpha=2$, the explicit implementation of the model causes no major problem, provided that the time step is controlled by the temperature variations between successive cycles. When we introduce electric fields into the model, α is close to unity and ω_{nl} behaves asymptotically as $v_T k$, which induces a CFL-like linear stability condition. This condition has proven to be difficult to fulfil rigorously in practical multigroup calculations where temperature over- (or under-) shoots are sometimes observed. Solutions that lay somewhere in between a full implicit or explicit resolution are suggested by the form given to the nonlocal flux, which appears as the sum of a local contribution and a correction for nonlocality:

$$\begin{aligned}\mathbf{Q}_{\mathrm{nl}}&=\frac{2\pi m_e}{3}\int_0^\infty \mathbf{f}_1^m v^5 dv-\frac{2\pi m_e}{3}\int_0^\infty \lambda_{ei}\nabla\,\Delta f_0 v^5 dv\\&=\mathbf{Q}_{\mathrm{local}}-\mathbf{Q}_{\mathrm{nl}}^{\mathrm{corr}}.\end{aligned}\tag{A.4}$$

In the implementation we use, the nonlocal correction is computed explicitly from the temperatures of the previous time step, whereas the local component is implicitly time differenced. This choice leads to the following finite difference energy equation:

$$\rho C_v\frac{T^{n+1}-T^n}{\Delta t}-\nabla\cdot(\kappa_{\mathrm{local}}^n\nabla T^{n+1})=\nabla\cdot[\mathbf{Q}_{\mathrm{nl}}^{\mathrm{corr}}]^n,$$

where the superscript n stands for the time $n\Delta t$. This implicit-explicit scheme allows us to retain the main features of the nonlocal model, and the implicit part of it is efficient in damping eventual overshoots caused by the explicit calculation. A simplified stability analysis may read as follows: The eigenvalues of the correction operator are $\omega_{\mathrm{corr}}=\omega_{\mathrm{SH}}-\omega_{\mathrm{nl}}$, so that the error amplification factor of the explicit phase is $1-(\omega_{\mathrm{SH}}-\omega_{\mathrm{nl}})\Delta t$. The amplification factor of the implicit local component is $[1+\omega_{\mathrm{SH}}\Delta t]^{-1}$. Thus, the amplification of the resulting scheme is $1-(\omega_{\mathrm{SH}}-\omega_{\mathrm{nl}})\Delta t/1+\omega_{\mathrm{SH}}\Delta t$: this number remains inferior to unity for any time step and the scheme is unconditionally stable. All computations presented here were carried out using this implementation.

[1] N. Meezan, L. Divol, M. Marinak, G. Kerbel, L. Suter, R. Stevenson, G. Slark, and K. Oades, Phys. Plasmas **11**, 5573 (2004).
[2] E. Epperlein and R. Short, Phys. Fluids B **4**, 2211 (1992).
[3] A. Sunahara, J. Delettrez, C. Stoeckl, R. Short, and S. Skupsky, Phys. Rev. Lett. **91**, 095003 (2003).
[4] Ph. Nicolaï, M. Vandenboomgaerde, B. Canaud, and F. Chaigneau, **7**, 4250 (2000).
[5] K. Shigemori, H. Azechi, M. Nakai, M. Honda, K. Meguro, N. Miyanaga, H. Takabe, and K. Mima, Phys. Rev. Lett. **78**, 250 (1997).
[6] A. Velikovich, J. Dahlburg, J. Gardner, and R. Taylor, Phys. Plasmas **5**, 1491 (1998).
[7] L. Spitzer and R. Härm, Phys. Rev. **89**, 977 (1953).
[8] J.-F. Luciani, P. Mora, and J. Virmont, Phys. Rev. Lett. **51**, 1664 (1983); J.-F. Luciani, P. Mora, and A. Bendib, *ibid.* **55**, 2421 (1985); J.-F. Luciani, P. Mora, and R. Pellat, Phys. Fluids **28**, 835 (1985).
[9] E. Epperlein and R. Short, Phys. Fluids B **3**, 3082 (1991).
[10] J. Albritton, E. Williams, I. Bernstein, and K. Swartz, Phys. Rev. Lett. **57**, 1887 (1986).
[11] S. Krasheninnikov, Phys. Fluids B **5**, 74 (1992).
[12] P. Mora and J.-F. Luciani, Laser Part. Beams **12**, 387 (1994).
[13] G. Schurtz, Ph. Nicolai, and M. Busquet, Phys. Plasmas **7**, 4238 (2000).
[14] W. Manheimer and D. Colombant, Phys. Plasmas **11**, 260 (2003); D.

Colombant, W. Manheimer, and M. Busquet, 12, 072702 (2005).
[15]S. Glenzer, W. Alley, K. Estabrook, J. De Groot, M. Haines, J. Hammer, J.-P. Jadaud, B. MacGowan, J. Moody, W. Rozmus, L. Suter, T. Weiland, and E. Williams, Phys. Plasmas **6**, 2117 (1999).
[16]S. Braginskii, in *Reviews of Plasma Physics*, edited by M. Leontovich (Consultants Bureau, New York, 1965) Vol. 1, p. 205.
[17]E. Epperlein and M. Haines, Phys. Fluids **29**, 1029 (1986).
[18]A. Bell, R. Evans, and D. Nicholas, Phys. Rev. Lett. **46**, 243 (1981).
[19]J. Albritton, Phys. Rev. Lett. **50**, 2078 (1983).
[20]E. Epperlein and R. Short, Phys. Fluids B **4**, 2211 (1992).
[21]J.-P. Matte, thesis, Ecole Polytechnique, France, 1987.
[22]R. Kingham and A. Bell, Phys. Rev. Lett. **88**, 045004 (2002).
[23]L. Bhatnagar, E. Gross, and M. Krook, Phys. Rev. Lett. **94**, 511 (1954); J. Green, Phys. Fluids **16**, 2022 (1973).
[24]J. Delettrez (private communication).
[25]V. Goncharov and G. Li, Bull. Am. Phys. Soc. **49**, 140 (2004).
[26]S. G. Bochkarev, V. Yu. Bychenkov, and W. Rozmus, Phys. Plasmas **11**, 3997 (2004).
[27]A. Bendib, J.-F. Luciani, and J.-P. Matte, Phys. Fluids **31**, 711 (1988).
[28]A. Brantov, V. Bychenkov, W. Rozmus, C. Capjack, and R. Sydora, Phys. Plasmas **10**, 4633 (2003).
[29]T. Kho, and M. Haines, Phys. Fluids **29**, 2665 (1986).
[30]J.-L. Feugeas, Ph. Nicolaï, and G. Schurtz (unpublished).
[31]R. Abgrall, J. Breil, P.-H. Maire, and J. Ovadia (unpublished).
[32]S. Atzeni, Plasma Phys. Controlled Fusion **29**, 1535 (1987).
[33]E. Epperlein, G. Rickard, and A. Bell, Phys. Rev. Lett. **61**, 2453 (1988).